

Supporting information

for

Metal-Metal Chalcogenide Molecular Precursors to Binary, Ternary, and Quaternary Metal Chalcogenide Thin Films for Electronic Devices

Ruihong Zhang[†], Seonghyuk Cho[‡], Daw Gen Lim[†], Xianyi Hu^{†§}, Eric A. Stach[§], Carol A. Handwerker[†], Rakesh Agrawal^{†}*

[†]School of Materials Engineering, Purdue University, West Lafayette, IN 47907, USA

[‡]School of Chemical Engineering, Purdue University, West Lafayette, IN 47907, USA

[§]Center for Functional Nanomaterials, Brookhaven National Laboratory, Upton, NY 11973, USA

Supporting information

Metal-Metal Chalcogenide Molecular Precursors to Binary, Ternary, and Quaternary Metal Chalcogenide Thin Films for Electronic Devices

Ruihong Zhang[†], Seonghyuk Cho[‡], Daw Gen Lim[†], Xianyi Hu^{†§}, Eric A. Stach[§], Carol A. Handwerker[†], Rakesh Agrawal^{‡}*

[†]School of Materials Engineering, Purdue University, West Lafayette, IN 47907, USA

[‡]School of Chemical Engineering, Purdue University, West Lafayette, IN 47907, USA

[§]Center for Functional Nanomaterials, Brookhaven National Laboratory, Upton, NY 11973, USA

EXPERIMENTAL METHODS

Dissolution of Pure Metals and Metal Chalcogenides

A series of dissolution experiments were performed by mixing Cu, Zn, Sn, In, Cu₂S, Cu₂Se, CuS, CuSe, SnS, SnSe, In₂S₃, In₂Se₃, Ag₂S, and Ag₂Se with butylamine (BA)/hexylamine (HA) and 1,2-ethanedithiol (EDT) (vol. ratio 1:1) at room temperature in a nitrogen-filled glovebox with both water and oxygen level <0.1 ppm. The sequence of adding solutions has no observable influence on the resulting solutions. The standard preparation sequence was: (i.) solid powders, (ii.) BA/HA, (iii.) EDT. It should be noted that none of the above powders dissolve in either primary amines or 1,2-ethanedithiol. The highest solubility (wt.%) of a metal or a metal chalcogenide in primary amine-dithiol solvent mixture was determined experimentally by observing how much bulk powders dissolved in a mixture of BA and EDT (vol. ratio of 1:1) at room temperature within ten days. Generally, gas bubbles are formed during the dissolution of metal powders in BA/HA-EDT solvent mixtures. For the dissolution rate, Zn metal dissolves faster than Cu and Sn metals; copper chalcogenides dissolve faster than tin chalcogenides. Also, dissolving the same amount of metals or metal chalcogenides takes shorter time in lower boiling point solvent mixtures. For example, the dissolution in BA-EDT is faster than in HA-EDT. Although the dissolution experiments were first performed inside a nitrogen-filled glovebox, we found that the above bulk powders except Cu and Ag₂Se could also be dissolved in BA/HA-EDT in air atmosphere. The colors of the resulting solutions are the same as that of corresponding solutions prepared in a nitrogen-filled glovebox.

Preparation of CZTSSe Precursor Solutions

The preparation of CZTSSe precursor solutions involves the formation of component solutions, and then the mixing of component solutions. The preparation of CZTSSe precursor solutions was performed in a N₂-filled glovebox. The detailed procedures for component solutions and precursor preparation are described as follows.

1) Component solutions for *Solution 1: CZTS precursors* were prepared as follows: *Solution A* (Cu₂S solution) was prepared by dissolving Cu₂S powder (0.210 g) in HA-EDT solvent mixture (vol. ratio of 1:1, 3 ml), forming a clear, dark brown solution after two days of stirring. *Solution B* (Zn solution) was prepared by dissolving Zn powder (0.103 g) in HA-EDT solvent mixture (vol. ratio of 1:1, 2 ml), yielding a clear, pink solution after few hours of stirring. *Solution C* (SnS solution) was prepared by dissolving SnS powder (0.0226 g) in HA-EDT solvent mixture (vol. ratio of 1:1, 5 ml), resulting in a colorless transparent solution after seven to ten days of stirring. *Solution 1* was prepared by mixing the above constituent solutions, and then diluted with HA at appropriate volume ratios, yielding a target concentration of [Sn]=0.1 M, and elemental ratios of [Cu]:[Zn]:[Sn]=1.76:1.05:1. Note that no sulfur solution was added during the preparation of the precursor solution, since 1,2-ethanedithiol and sulfides supplied the sulfur during the film formation. The as-formed solution has a clear brown color and stable for months.

2) Component solutions for *Solution 2: CZTSSe precursor* were prepared as follows: *Solution A'* (Cu₂Se solution) was prepared by dissolving Cu₂Se powder (0.244 g) in a mixture of HA-EDT solvent mixture (vol. ratio of 1:1, 3 ml), forming a clear, dark red solution after two days of stirring. *Solution B'* (Zn solution) was formed by dissolving Zn powder (0.103 g) in HA-EDT solvent mixture (vol. ratio of 1:1, 2 ml). *Solution C'* (SnSe solution) was prepared by dissolving SnSe powder (0.297 g) in HA-EDT solvent mixture (vol. ratio of 1:1, 5 ml), resulting in a clear, orange solution after seven to ten days of stirring. *Solution D'* (S solution) was prepared by dissolving S (0.385 g) and Se (0.948 g) in HA-EDT (vol. ratio of 1:1, 6 ml). *Solution 2* was prepared by mixing the above constituent solutions at appropriate quantities and then diluted with HA, yielding a target concentration of [Sn]=0.1 M, and elemental ratios of [Cu]:[Zn]:[Sn]:[S]:[Se]=1.45:1.05:1:2:2. The as-formed solution has a transparent red color and stable for months. It should be noted that the solvent mixture in *Solution 1* and *Solution 2* sometimes crystallize at room temperature; vortexing or stirring will reverse the crystallization. The crystallization of the solvent mixture has been demonstrated by mixing HA and EDT at volume ratio of 1:1 without the addition of solute.

3) Component solutions for *Solution 3: CZTSSe precursor* were prepared as follows: *Solution A''* (Cu solution) was prepared by dissolving Cu powder (0.092 g) in a mixture of HA-EDT solvent

mixture (vol. ratio of 1:1, 4 ml), forming a clear, light red solution after three days of stirring. *Solution B* (Zn solution) was formed by dissolving Zn powder (0.069 g) in a mixture of HA-EDT solvent mixture (vol. ratio of 1:1, 2 ml). *Solution C* (Sn solution) was prepared by dissolving Sn powder (0.119 g) in a mixture of HA-EDT solvent mixture (vol. ratio of 1:1, 5 ml), resulting in a clear pink, solution after five to seven days of stirring. *Solution D* (S solution) was prepared by dissolving S (0.385 g) and Se (0.948 g) in HA-EDT solvent mixture (vol. ratio of 1:1, 6 ml). *Solution 3* was prepared by mixing the above constituent solutions at appropriate quantities, yielding a target concentration of $[\text{Sn}] = 0.1 \text{ M}$, and elemental ratios of $[\text{Cu}]:[\text{Zn}]:[\text{Sn}]:[\text{S}+\text{Se}] = 1.45:1.05:1:5$. The solution is a transparent red color and stable over months.

Deposition of Multinary Chalcogenide Thin Films

Precursor films were deposited by spin coating the precursor solutions on molybdenum-coated soda lime glass. For the deposition of binary thin films, the substrates were first flooded with the corresponding binary precursors and then spun at 800 rpm for 30 sec. For the deposition of CZTSSe precursor films, the spin coating process is programmed at 500 rpm for 5 sec and 1500 rpm for 25 sec. After the deposition of each precursor layer, the thin film was annealed at $\sim 300^\circ\text{C}$ for 5 min. These steps were repeated until the desired thickness was acquired. Then, the thin film was further annealed at 500°C in a selenium atmosphere for 30 min to achieve a large-grained morphology. The selenization condition is described in previous publications.¹⁻³

Thin Film Characterization

Grazing incident X-ray diffraction (GIXRD) data were collected using a Rigaku diffractometer (Cu K_α radiation, 0.154 nm wavelength) with parallel-beam mode. Raman spectra were gathered from HORIBA Jobin Yvon LabRam HR800 system with an excitation wavelength of 633 nm. The thin film morphology and compositions were characterized using a FEI Quanta scanning electron microscopy (SEM) equipped with energy dispersive X-ray spectroscopy (EDX) (Oxford Aztec Xstream-2 silicon drift detector, SDD). FIB-lift off samples were processed in FEI Helios, and then characterized with 200-kV Hitachi 2700C equipped with Bruker SDD EDX.

Solar Cell Fabrication and Characterization

The CZTSSe absorbing layer was fabricated based on the direct solution route. The material layers from the bottom to the top of a complete device are: soda lime glass (SLG, $\sim 2 \text{ mm}$), fiber-textured molybdenum film (Mo, $\sim 800 \text{ nm}$), chemical bath deposited cadmium sulfide (CdS, ~ 50

nm), sputtered intrinsic zinc oxide (ZnO, ~80 nm) and tin-doped indium oxide (ITO, ~220 nm), and e-beam deposited Ni/Al metal contacts. A ~100 nm antireflective magnesium fluoride (MgF₂) coating was applied on the cell prepared from *Solution 2*. The J-V characteristics were measured with a four-point probe station using a Keithley 2400 series sourcemeter and a Newport Oriel simulator with AM 1.5 illumination. The solar simulator was calibrated to 100 mW/cm² using a Si reference cell certified by NIST.

RESULTS

Solutions in Primary Amine-dithiol Mixtures: Table S1 summarizes the metals and metal chalcogenides, which are soluble in the primary amine-monothiol/dithiol solvent mixtures. The primary-monothiol solvent mixture cannot dissolve these metals and metal chalcogenides except zinc powders (≤ 0.1 M). The primary amine-dithiol solvent mixture can dissolve many metals and metal chalcogenides in both inert and air atmospheres at room temperature (Fig. S1).

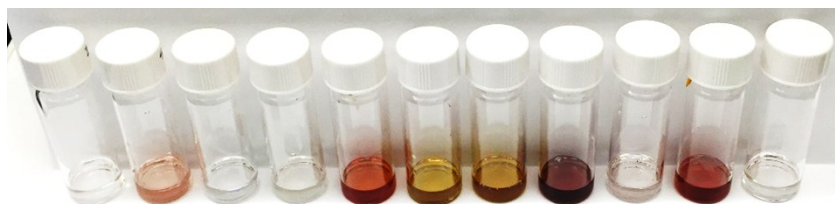


Fig. S1 Solutions of Zn, Sn, In, SnS, SnSe, CuS, Cu₂S, Cu₂Se, In₂S₃, In₂Se₃, and Ag₂S (left to right) prepared in HA-EDT solvent mixtures at room temperature in air atmosphere. The solution concentrations are 0.2 M.

Table S1 Dissolution of Metals and Metal Chalcogenides.

Bulk Material	BA/HA	BA/HA-PT BA/HA-ET	BA/HA-EDT		Color
			Air	N ₂	
Metal					
Cu				√	Clear, dark yellow
Zn		√	√	√	Clear, light pink
Sn			√	√	Clear, pink
In			√	√	Clear, colorless
Metal Chalcogenide					
CuS			√	√	Clear, dark yellow
Cu ₂ S			√	√	Clear, dark yellow
CuSe			√	√	Clear, yellow
Cu ₂ Se			√	√	Clear, red
SnS			√	√	Clear, colorless
SnSe			√	√	Clear, orange
In ₂ S ₃			√	√	Clear, light pink
In ₂ Se ₃			√	√	Clear, red
Ag ₂ S			√	√	Clear, colorless
Ag ₂ Se				√	Clear, yellow

BA: butylamine; HA: hexylamine; PT: propanethiol; ET: ethanethiol; EDT: 1,2-ethanedithiol

Conductivity Measurement: Table S1 shows the conductivities of BA, HA, EDT, BA-EDT (vol. ratio 1:1; molar ratio 1:1.18), HA-EDT (vol. ratio 1:1; molar ratio 1:1.57), and the binary solvent mixtures with different zinc concentrations ($[Zn]=0.3\sim 0.7$ mol/L). The electrolytic conductivity measurements on all the solvents and solutions were performed at 25°C. The electrolytic conductivity of BA, HA, and EDT was measured first. Then, BA/HA and EDT were mixed homogenously for the measurements of solvent mixtures. The solutions with different Zn concentrations were prepared by dissolving increasing amount of Zn metal in the same solvent mixture. Conductivity measurements were performed as soon as clear solutions formed.

Table S2 Conductivities of solvents and Zn solutions at room temperature.

Solvent	Zn Concentration (mol/L)	Conductivity ($\mu\text{S}/\text{cm}$)
Butylamine (BA)	N/A	0
Hexylamine (HA)	N/A	0
1,2-Ethanedithiol (EDT)	N/A	0
BA-EDT (vol. ratio 1:1)	0	1926.5
BA-EDT (vol. ratio 1:1)	0.3	1500.8
BA-EDT (vol. ratio 1:1)	0.5	1274.4
BA-EDT (vol. ratio 1:1)	0.7	960.7
HA-EDT (vol. ratio 1:1)	0	550.2
HA-EDT (vol. ratio 1:1)	0.3	502.0
HA-EDT (vol. ratio 1:1)	0.5	428.6
HA-EDT (vol. ratio 1:1)	0.7	327.7

Deposition of Zn Solutions: The as-dried and as-annealed films from the Zn solution were characterized using GIXRD (Fig. S2). The amorphous precursor film converted to ZnS, with a mixture of zincblende (F-43m) and wurtzite ZnS (P63m), after annealing at 300°C for 10 min. This indicated that EDT supplied sulfur for the formation of ZnS. When sulfur was also provided externally by adding a sulfur solution into the zinc solution ($[Zn]:[S]=1:1.25$), the crystallinity of the film was improved, and both zincblende and wurtzite ZnS were formed.

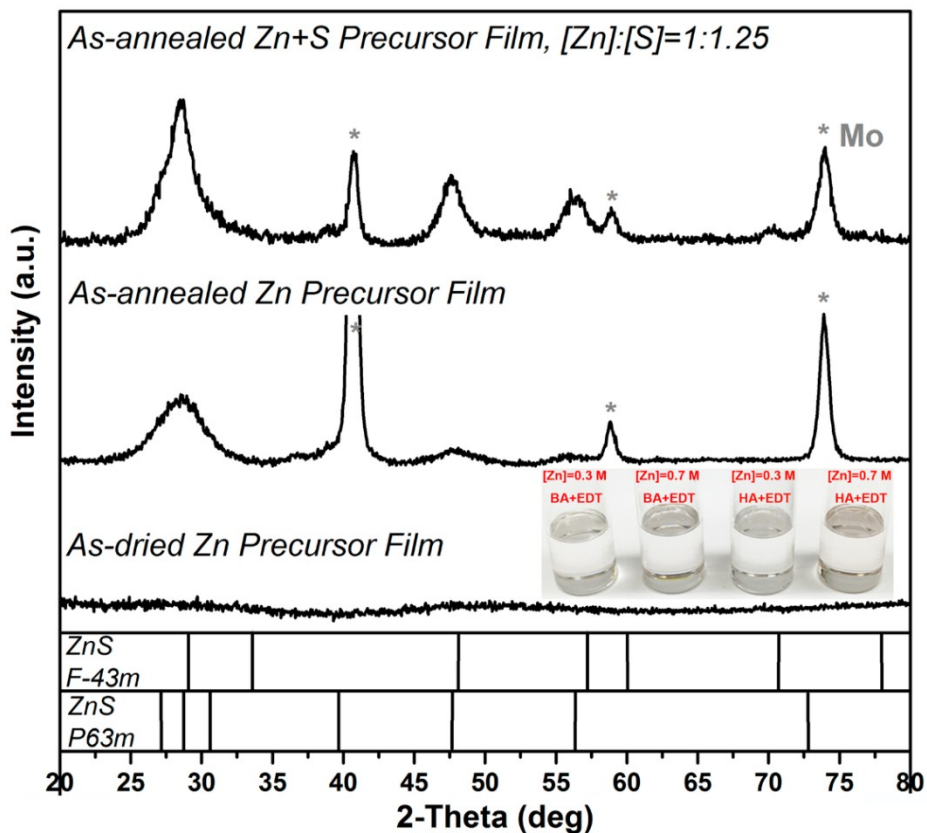


Fig. S2 GIXRD patterns for the as-dried Zn precursor film, as-annealed Zn precursor film, and as-annealed Zn+S precursor film. The inset is Zn solutions with concentrations of 0.3 and 0.7 M.

Thermal Gravimetric Analysis (TGA): TGA was performed on a TA Instrument Q50 with an alumina crucible under a flowing nitrogen atmosphere. For the measurement, the following heating program was employed: isothermal at room temperature for 20 min, ramp 10°/min to 500°C with a nitrogen flow 60 mL/min. The sample sizes of ~10 mg was analyzed for SnS solution (HA-EDT, 0.3 M). The end temperature of phase transformation is 300°C, corresponding to the annealing temperature used in this study (Fig. S3).

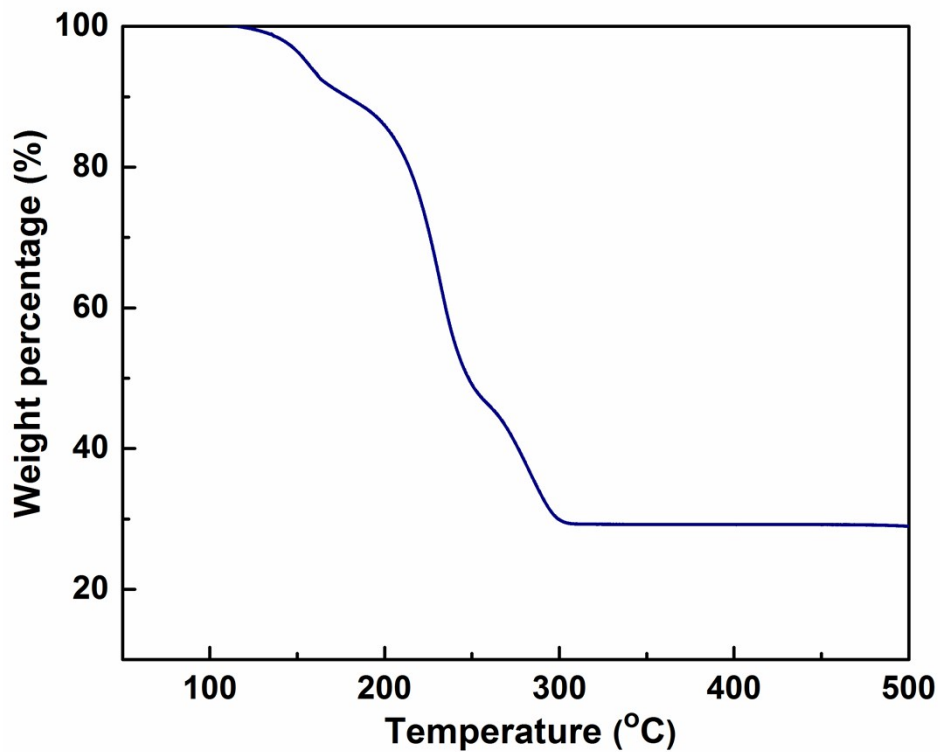


Fig. S3 TGA trace of SnS solution.

CZTS Film Deposition from *Solution 1*: The annealed CZTS precursor film is flat and smooth over a large area (Fig. S4a). The total thickness is around 800 nm for an 8-layer coating, with each precursor layer densely packed onto the Mo substrate (Fig. S4b). The GIXRD and Raman spectrum in Fig. S4e and S4f reveal that the precursor film consists of kesterite CZTS nanoparticles. The formation of kesterite CZTS phase at this low temperature is attributed to the low formation energy of this quaternary phase and the compositional homogeneity of the precursor film. After selenization at 500°C for 40 min, large grains with layered structure were formed (Fig. S4b and d). As shown in Fig. S4e, the sharp peaks in GIXRD pattern are aligned with kesterite CZTSe phase with a slight high angle shift. In the Raman spectrum (Fig. S4f), the peak at 173, 197, 234, and 247 cm^{-1} correspond to kesterite CZTSe phase, while the small, broad peak at 328 cm^{-1} is attributed to the vibration of S atoms in the lattice,⁴ indicating the existence of residual S atoms in the lattice after the selenization.

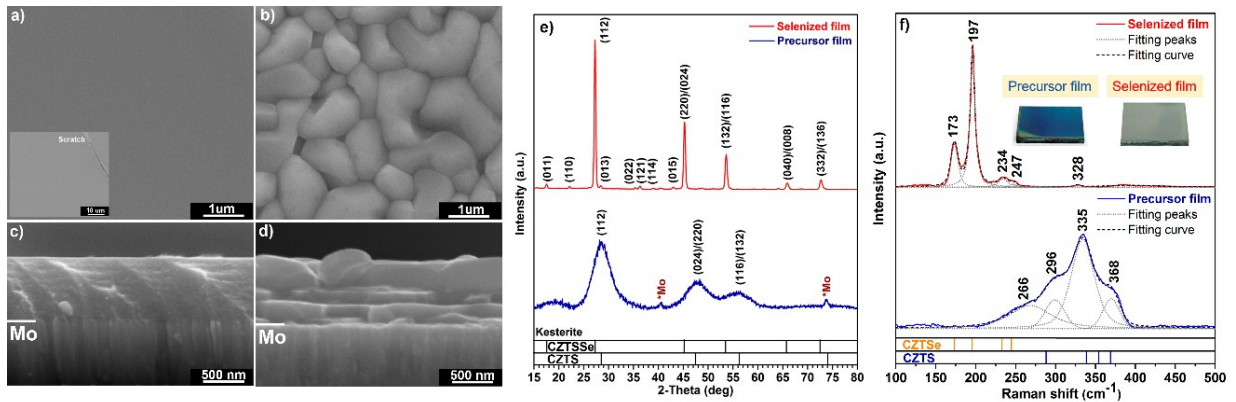


Fig. S4 SEM images, GIXRD patterns, Raman spectra of a precursor film and a selenized film prepared from *Solution 1*: CZTS precursor. a) and c) top-view and cross-sectional SEM images of a precursor film. b) and d) top-view and cross-sectional SEM images of a selenized film. Inset in a) is a low-magnification top-view image of the precursor film. A scratch was intentionally put on the surface to facilitate focusing of the microscope. e) GIXRD patterns and f) Raman spectra of the selenized film and the precursor film.

CZTSSe Film Deposition from *Solution 2*: Fig. S5a and b are the top-view and cross-sectional SEM images of CZTSSe film deposited from *Solution 2*. Fig. S5c and Table S2 show EDX results and composition ratios of Cu/Zn+Sn, Zn/Sn, and S+Se/Sn in the precursor solution, the precursor film, and the selenized film. The composition of the selenized film is $\text{Cu}_{1.90}\text{Zn}_{1.18}\text{Sn}_1(\text{S}_{0.07},\text{Se}_{0.93})_{4.12}$. The increase in Zn/Sn and Cu/(Zn+Sn) ratios indicate the loss of tin during heat treatment.

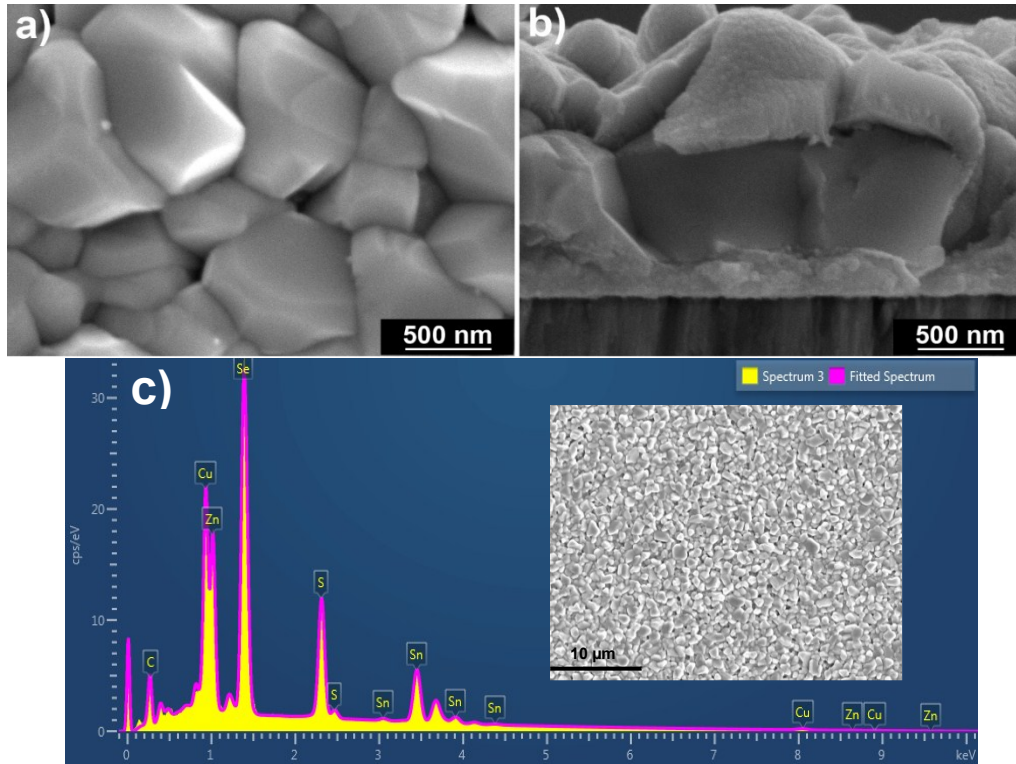


Fig. S5 SEM images and EDX spectrum of the selenized CZTSSe film. a) Top-view, b) Cross-sectional of a device, and c) EDX spectrum.

Table S3 Average composition in the precursor solution, precursor film, and selenized film.

Atomic ratio	Solution	Precursor film	Selenized film
[Cu]/[Zn+Sn]	0.71	0.73	0.87
[Zn]/[Sn]	1.05	1.15	1.18
[S]+[Se]/[Sn]	4	3.98	4.12

High-resolution STEM-HAADF:

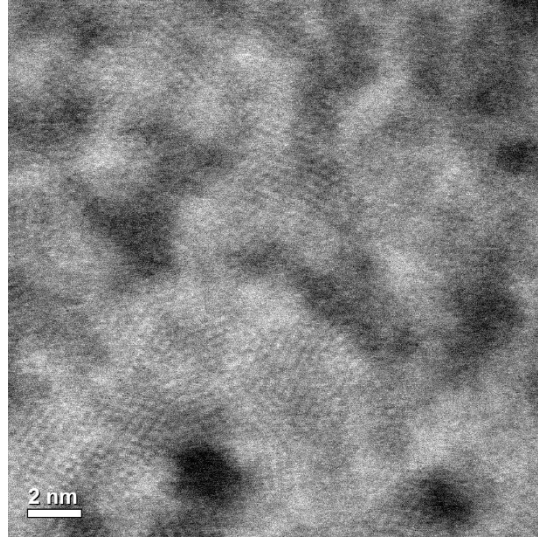


Fig. S6 High-resolution STEM-HAADF image of nanoparticles in the precursor film prepared from *Solution 2*.

J-V Characteristics of a Solar Cell Processed from *Solution 3*: Pure metals (Cu, Zn, and Sn) and chalcogens (S and Se) were used in this precursor solution. Fig. S7 shows the J-V characteristics of a solar cell processed from *Solution 3*. The continual optimization in the film thickness and composition will improve the efficiencies.

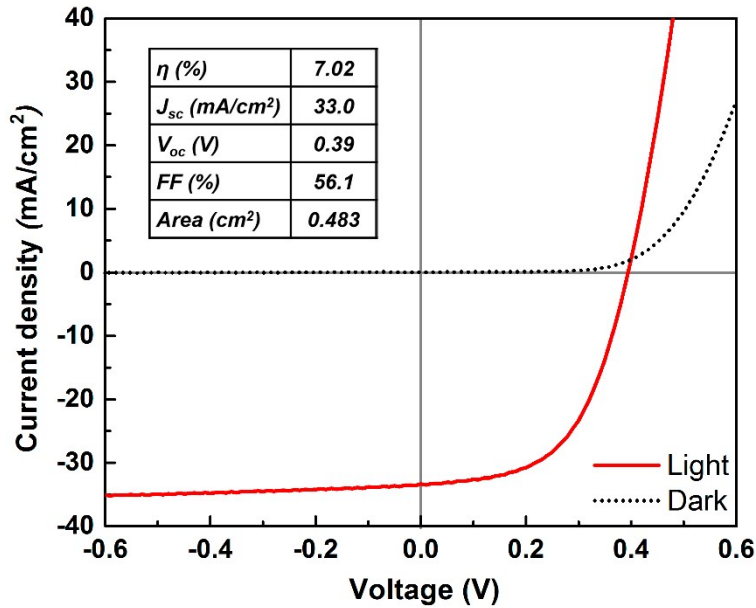


Fig. S7 J-V curves for the solar cell processed from *Solution 3*: *pure-metal precursor*. The dotted line shows the dark current density, while the solid line represents the light current density.

REFERENCES

- (1) C. J. Hages, S. Levenceno, C. K. Miskin, J. H. Alsmeier, D. Abou-Ras, R. G. Wilks, M. Bär, T. Unold and R. Agrawal, Progress in Photovoltaics: Research and Applications, **2015**, 23, 376.
- (2) N. J. Carter, W. C. Yang, C. K. Miskin, C. J. Hages, E. A. Stach and R. Agrawal, Solar Energy Materials and Solar Cells, **2014**, 123, 189.
- (3) R. Zhang, S. M. Szczepaniak, N. J. Carter, C. A. Handwerker and R. Agrawal, Chem Mater, **2015**, 27, 2114.
- (4) M. Grossberg, J. Krustok, J. Raudoja, K. Timmo, M. Altosaar and T. Raadik, Thin Solid Films, **2011**, 519, 7403.